ELSEVIER

Chemical Engineering Science 62 (2007) 3443–3454

Chemical Engineering Science

www.elsevier.com/locate/ces

Multiscale phenomena in microfluidics and nanofluidics

Guoqing Hu, Dongqing Li*

Department of Mechanical Engineering, Vanderbilt University, Nashville, TN 37235-1592, USA

Received 9 June 2006; received in revised form 14 November 2006; accepted 17 November 2006
Available online 23 March 2007

Abstract

A lab-on-a-chip device typically integrates many microfluidic components and has similar functions to the room-sized laboratory. However, developing such a lab-on-a-chip device is not simply to scale down the conventional instruments. It requires the understanding and controlling of many multiscale physical and chemical phenomena, spanning from centimeter to nanometer. In this paper, we provide an overview of the multiscale fluidic phenomena encountered in lab-on-a-chip devices, with focus on electrokinetics. We review different computational models for the studies of microfluidics and nanofluidics. Several application examples using microfluidics and nanofluidics, including micromixing, particle/cell separation, and DNA separation, are given.

Keywords: Lab-on-a-chip; Multiscale; Electrokinetics; Microfluidics; Nanofluidics; Computer simulation

1. Introduction

Size generally means the physical dimensions, proportions, magnitude, or extent of an object. In the real world, length is one of the most important dimensions of measurement, spanning from 10^{25} m (our entire universe) down to 10^{-16} m (lepton and quark). Many fundamental processes of biology, however, do not cover quite as large a range of sizes as mentioned above. For instance, translation, gene regulation, and cell communication occur on the micrometer to nanometer scale (Tegenfeldt et al., 2004). Table 1 lists the typical length scales of some of the biological objects. In order to study the various biological phenomena and processes at the molecular level and at the cellular level, researchers must be able to access these relevant length scales. This requires the experimental devices to have characteristic sizes of a few nanometers up to several micrometers. During the past decade, micromachining and microfabrication technology has become available to make nano- and micron-sized devices, thus enabling studies of objects with these length scales.

Since Manz et al. (1990) developed the concept of miniaturized total analysis system (μ TAS) or lab-on-a-chip, the miniaturization of biological or chemical devices has attracted substantial attention and remarkable progress has been achieved (refer to the reviews by Reyes et al., 2002; Auroux et al., 2002; Erickson and Li, 2004). An integrated lab-on-a-chip device can incorporate many of the necessary components and functionality of a typical room-sized laboratory into a small chip that performs a specific biological or chemical analysis, including sample treatment, transport, reaction, and detection. Originally it was thought that the most significant benefit of the miniaturization would be the analytical improvements associated with the scaling down of the size (Manz et al., 1990). Further development revealed other advantages such as minimized reagents, increased automation, and reduced manufacturing costs (Kock et al., 2000).

Lab-on-a-chip devices are not just a simple smaller version of the conventional instruments. Miniaturization raises many new challenges. Fluid and sample transport is a crucial issue in these lab-on-a-chip devices because many biological and chemical processes and experiments take place in aqueous environments. The fundamental properties of fluid in micro/nanoscale may differ significantly from those in larger devices. For gaseous flows, the continuum Navier–Stokes equations are valid only if the Knudsen number $Kn < 0.1$, while the non-slip

* Corresponding author. Tel.: +1 615 3228601; fax: +1 615 3436687.
E-mail address: dongqing.li@vanderbilt.edu (D. Li).

0009-2509/$ - see front matter © 2007 Elsevier Ltd. All rights reserved.
doi:10.1016/j.ces.2006.11.058

Table 1
Length scale of typical objects in biology

Diameter of glucose molecule	1 nm
Diameter of DNA helix	2 nm
Diameter of insulin molecule	5 nm
Thickness of cell wall (gram negative bacteria)	10 nm
Size of typical virus	75 nm
Diameter of the smallest bacterium	200 nm
Diameter of red blood cell	8.4 μm
Diameter of average cell in human body	10 μm
Diameter of the largest bacterium	750 μm

boundary condition holds for the stricter limit of $Kn < 0.001$. For liquid flows, the fluidic phenomena in microscale (100 nm $\sim$ 100 μm) still can be described by the continuum theory but the decrease of length scale makes surface force and electrokinetic effects important and inertial force unimportant. One of the well-known examples is that mass transportation in microfluidic device is normally dominated by viscous force rather than inertial force. Dimensions of fluidic channels continue to be scaled down to below 100 nm, entering the region of nanofluidics. The liquid can no longer be fully considered as a continuum but as an ensemble of individual molecules. In these scales, the surface-to-volume ratio is very high, the non-slip boundary condition does not hold fully, and fluid constitutive relations are strongly affected by the existence of the boundary. The study of micro/nanoscale fluid mechanics is important for the understanding and development of the lab-on-a-chip devices at the corresponding scales.

The fluid motion in microfluidics and nanofluidics is generated typically by applying a pressure difference to a channel or by applying an electric field along the channel. Pressure-driven flow has in general a parabolic flow profile that may degrade separation efficiency. Moreover, very large hydrodynamic pressure is required to generate liquid flow in microfluidic and nanofluidic devices since the hydraulic resistance is reversely proportional to the fourth power of transverse channel dimension, which makes many designs using pressure - driven flow impractical. An alternative to pressure-driven flow is electrokinetic pumping that is easy to control and is insensitive to channel sizes compared to pressure-driven flow (Probstein, 1994; Li, 2004). The advantage of electrokinetic pumping is that the flow is plug-like and independent of the size of the channels provided that the diameter of channel $\gg$ Debye length (1 $\sim$ 10 nm for standard buffer conditions). Electrokinetic mechanisms, including electroosmosis, electrophoresis, and (AC and DC) dielectrophoresis, are playing more and more important roles in micro/nanoscale devices. They have been extensively used for flow control (Hu et al., 2005), micromixing (Erickson and Li, 2003; Biddiss et al., 2004), concentration gradient generation (Lee et al., 2005), separation (Kang et al., 2006), sorting (Xuan and Li, 2005), and DNA detection (Paegel et al., 2002) on lab-on-a-chip platforms.

Along with experimental and theoretical studies, numerical simulation has been an indispensable tool in almost every research and application field for many years. It also provides great help in the design of microfluidic and nanofluidic devices (Erickson, 2005). Simulations allow researchers to rapidly determine how design change will affect chip performance, thereby reducing the number of prototyping iterations. However, there are several factors that complicate the numerical simulation of micro/nanoscale phenomena and thus distinguish it from the macroscale counterpart. The first and most important one is the large range of relevant length scales, which can vary up to seven orders (from Debye layer, nm, to channel length and substrate thickness, cm). Secondly, the downscaling of the size dramatically increases the relative importance of surface and interfacial phenomena. Rapid and localized changes of fluidic and material properties often occur in the miniature devices. Another challenge in numerical simulation is the intrinsic multiphysics phenomena that usually combine less or more fluid mechanics, heat transfer, electrokinetics, chemical and biological thermodynamics, and reaction kinetics. In general, one must consider all these aspects in order to provide a numerical picture for a true lab-on-a-chip device.

In this paper, we first discuss the fundamental electrokinetic phenomena and then give an overview of some of the most important scale parameters in microfluidics and nanofluidics. We will continue to review the theoretical and numerical models employed in micro/nanoscales. Finally, we will focus on application-based devices and prototypes using microfluidics and nanofluidics.

2. Electrokinetics in microfluidics and nanofluidics

2.1. Electroosmosis

Generally, the solid surfaces of microchannel acquire electrostatic charges when they are in contact with an aqueous solution. The surface charge in turn attracts the counter-ions in the liquid to the region close to the surface, forming the electric double layer (EDL). Under a tangentially applied electric field, the excess counter-ions in the double layer region will move, resulting in a bulk liquid motion via viscous effect. This is known as the electroosmotic flow (Russel et al., 1989; Probstein, 1994; Ghosal, 2004; Li, 2004). The electroosmotic flow of incompressible liquids can be described by the Navier–Stokes equations,

$$\rho(\partial_t \mathbf{u} + \mathbf{u}\cdot\nabla\mathbf{u}) = -\nabla p + \mu\nabla^2\mathbf{u} - \rho_e\nabla\phi,$$
$$\nabla\cdot\mathbf{u} = 0, \tag{1}$$

where $\mathbf{u}$ is the flow velocity vector, ρ is the fluid density, μ is the fluid viscosity, p is the pressure, ρ_e is the net charge density, and ϕ is the electric potential. ρ_e is related to the potential ϕ by the Poisson equation,

$$\varepsilon\nabla^2\phi = \rho_e, \tag{2}$$

where ε is the dielectric constant of the fluid medium. In the absence of a significant convective or electrophoretic disturbance to the double layer, the charge density can be described by a Boltzmann distribution (Hunter, 1981),

$$\rho_e = -2zen_0\sinh(ze\phi/k_bT), \tag{3}$$

where z is the valence, e is the charge of an electron, n_0 is the bulk electrolyte concentration, k_b is the Boltzmann constant, and T is the temperature. Combining Eqs. (2) and (3) yields the non-linear Poisson–Boltzmann distribution equation,

$$\nabla^2\phi - \kappa^2 \sinh(\phi) = 0, \tag{4}$$

where κ is a constant determined by the ionic composition of the electrolyte (Russel et al., 1989).

Only for simple one-dimensional case, there is an analytical solution to the non-linear Poisson–Boltzmann equation (Burgreen and Nakache, 1964). For multidimensional complex geometries, Eq. (4) must be solved numerically. In the interest of developing an analytical solution, Eq. (4) can be linearized using Debye–Hückel approximation (Hunter, 1981),

$$\nabla^2\phi - \kappa^2\phi = 0. \tag{5}$$

In general, Eq. (5) is considered valid only when $\phi \ll k_b T/e$ (about 26 mV at room temperature).

Debye length ($\lambda_D = 1/\kappa$) is the characteristic thickness of the EDL, and is defined by the equilibrium distribution of mobile ions in the diffused part of the double layer field. According to the theory of the EDL, the equilibrium distribution of mobile ions in the diffused part of the double layer field, the Poisson–Boltzmann distribution, is determined by the random thermal motion of the ions and the electrostatic interaction between the ions and the charged surface. The Debye length ranges from several nanometers to several hundreds namometers, depending on the bulk ionic concentration. For flow in nanochannels, the channel's size may be comparable or smaller than the Debye length. There is significant overlap of the electrostatic fields from the different sides of the charged channel wall. The ion distribution no longer obeys the Poisson–Boltzmann distribution. Mass transport by electroosmotic convection and ionic conductance in nanofluidic systems significantly deviates from micrometer-sized systems because the electric potential barrier from relatively large EDL strongly influences concentration distribution and transport properties of ionic species. Molecular dynamics simulation has been applied to study both the flow and ion distribution in nanochannels (Qiao and Aluru, 2002). In addition, continuum approach can also be applied to flows in relatively large nanochannels (Taylor and Ren, 2005; Ren and Li, 2005). If the channel height h is not too small (i.e., $\lambda_D/h \ll 1$), the electric potential decays from the effective surface potential (ζ potential) to zero in the fluid away from the EDL. Therefore, for most microfluidic applications, the thickness of the EDL can be neglected in the study of electroosmotic flows (thin EDL approximation). The coupled system of the Navier–Stokes and Poisson–Boltzmann equations can be significantly simplified under this approximation: the term $-\rho_e\nabla\phi$ can be dropped from Eq. (1), instead, at channel surfaces, the no-slip boundary condition is replaced by an effective Helmholtz–Smoluchowski slip boundary (Anderson, 1989). Many researchers have applied this simplified approximation in the study of electroosmosis in microscale (Santiago, 2001; Ren et al., 2003; Zhang et al., 2006). The new development in this line is that a non-uniform zeta potential is introduced to enhance the mixing efficiency. The mixing enhancement was experimentally observed (Herr et al., 2000) and numerically demonstrated (Erickson and Li, 2003). This can be analytically understood when a heterogeneous zeta potential can generate secondary electroosmotic flows and thus transport reactants more efficiently (Zhang et al., 2006).

2.2. Electrophoresis and dielectrophoresis

Electrophoresis refers to the motion of a charged particle relative to the surrounding liquid under an applied electric field. When a charged colloidal particle or molecule suspended in an electric field, it will experience a lateral electric force (Johns and Washizu, 1996; Gascoyne and Vykoukal, 2002),

$$\bar{F}_e = q\bar{E} + (\bar{m}\nabla)\bar{E} + \tfrac{1}{6}\nabla(\vec{Q} : \nabla\bar{E}) + \cdots. \tag{6}$$

The first term describes the electrophoretic phenomena caused by the coulombic interaction between the net charge q of the particle or molecule and the electric field $\bar{E}$. This force is responsible for electrophoresis. Capillary electrophoresis (CE) was originally used to separate the hundreds of different species in narrow tubes, followed by detections (absorbance, fluorescence, electrochemical, mass spectrometry, and so on). Due to its variability and ease for automation, CE has been integrated with microfluidic devices mainly for DNA separation and diagnosis (Schmalzing et al., 2000; Tian et al., 2001; Xu et al., 2002). CE separates the analytes based on the difference of the electrophoresis mobility that depends on net charge and frictional forces (size/molecular weight of the analytes).

The other terms in Eq. (6) arise from the interaction of dielectric polarization of the particle or molecule by the inhomogeneous electric field. These polarization forces can generate motion of particles without surface charge in a non-uniform electric field. Such a motion is called dielectrophoresis (DEP). As described by Pohl (1978), the electric field can be produced by either a direct current (DC) or alternating current (AC). The only requirement is that field be non-uniform. Using DEP, manipulation of particles can be realized by controlling the electric field without any mechanical moving part. Furthermore, in contrast to the conventional electrophoresis that works only on the charged particles, DEP functions with both electrically neutral or charged particles, which greatly increases its biological applicability. DEP has been used in electric manipulation of micro-/nano-sized objects such as whole cells, DNA, virus particles, and naontubes. However, some considerations should be taken into account for the DEP applications in micro/nanoscales. The magnitude of the DEP force is dependent on the size and dielectric property of the particle. As the particle size decreases, DEP force on the particle decreases. Meanwhile, it is well known that the intensity of Brownian motion increases as particles become smaller. DEP force must dominate the Brownian motion to build up deterministic motion of the manipulation of the submicrometer objects. Thus scaling of DEP and Brownian motion with object size and channel geometry is crucial, especially at the nanometer scale.

2.3. Non-linear electrokinetics

The bulk electroosmosis flow is generated by the interaction of the tangentially applied DC electric field with the net charge in the EDL. In many situations, the thickness of the EDL is small compared to the channel transverse geometry. The effective slip velocity at the solid–liquid interface can be described by Helmholtz–Smokuchowshi formula,

$$\bar{u}_{\text{slip}} = -\frac{\varepsilon\zeta}{\mu}\bar{E} \tag{7}$$

in terms of the permittivity ε and viscosity μ of the liquid and the zeta potential ζ. This slip velocity is linear with respect to the electric field and thus the related phenomena are called linear electrokinetics. If the ζ is constant everywhere and there is no internal pressure gradient, the electroosmotic velocity is proportional to the electric field everywhere (Morrison, 1970; Cummings et al., 2000). One of drawbacks from such linearity is that the electroosmosis flow is somewhat weak. For example, to get 1 mm/s velocity of an aqueous solution with $\zeta = 10$ mV requires an electric field of 1400 V/cm. The high voltages not only need expensive high voltage power supply but also bring out Joule heating effect that is often unfavorable in applications (Ross et al., 2001; Xuan et al., 2004).

Recently there is an increasing interest in various non-linear and non-equilibrium electrokinetic phenomena, including AC electroosmosis (Ajdari, 2001), induced-charge electroosmosis (Bazant and Squires, 2004), and superfast electrophoresis (Barany et al., 1998; Ben et al., 2004). The basic principle that unifies all of these phenomena is to induce non-uniform polarization within the EDL with the external electric field or with the motion it drives. The normal external field must be significant compared to the surface field within the EDL to invoke these phenomena. As a result, the zeta potential ζ is not fixed, but rather changes in response to the external electric field. Dukhin (1991) studied the flows around a conducting ion selective granule in a uniform electric field within an electrolyte and estimated the average non-linear electroosmotic velocity as

$$u = -\varepsilon E^2 R/\mu, \tag{8}$$

where R is the radius of the granule. For $R = 1$ mm and $E = 100$ V/cm, the effective ζ potential (ER, analogical to ζ in Eq. (7)) can be as large as 10 V, far greater than the normal ζ potential ($10 \sim 100$ mV). Therefore, the electroosmosis and electrophoresis velocity may be greater by 1 or 2 orders of magnitude than those predicted by linear formula. Barany et al. (1998) experimentally measured non-linear electrokinetic velocities in excess of 1 cm/s, much larger than standard electroosmotic
velocity. The non-linear electrokinetic flow was also used to enhance micromixing by generating microvortex around the conducting particle (Ben and Chang, 2002; Wang et al., 2004).

2.4. Some issues of fluid mechanics

Fluid flow in small devices acts differently from those in macroscopic scale. There are several excellent comprehensive reviews on fluid mechanics in micro/nanoscale (Gad-el-Hak, 1999; Stone et al., 2004; Squires and Quake, 2005). Here we only address some aspects that we believe are important to electrokinetic phenomena.

The Reynolds number (Re) is the most often mentioned dimensionless number in fluid mechanics. The Re number, defined by $\rho U L/\mu$, represents the ratio of inertial forces to viscous ones. In most circumstances involved in micro- and nanofluidics, the Re number is at least one order of magnitude smaller than unity, ruling out any turbulence flows in micro/nanochannels. Inertial force plays an insignificant role in microfluidics, and as systems continue to scale down, it will become even less important. For such small Re number flows, the convective term ($\rho\mathbf{u}\cdot\nabla\mathbf{u}$) of Navier–Stokes equations can be dropped. Without this non-linear convection, simple micro/nanofluidic systems have laminar, deterministic flow patterns. They have parabolic velocity profile in pressure-driven flows, plug-like velocity profile in electroosmotic flows, or a superposition of both. One of the benefits from the low Re number flow is that genomic material can be transported easily without shearing in lab-on-a-chip devices. It is worth noting, however, that other mechanisms, such as capillary effects, viscoelasticity, and electrokinetic effects may complicate the flow phenomena since their non-linearity increases in small scales (Squires and Quake, 2005).

Rapid mixing of the different analytes is crucial in many of the lab-on-a-chip systems. Biological processes, such as cell culture, immunoassay, and DNA hybridization, often require mixing of reactants to achieve good reaction kinetics. In contrast to the macroscale mixing that can be enhanced by turbulence or chaotic advection, mixing in the microscale devices mainly depends on the molecular diffusion, resulting in an unacceptably slow process even in small scale. For example, for an analyte diffusion coefficient of $D = 10^{-10}$ m^2/s (for protein and many biomolecules), the docking time $\tau_D = w^2/D$ is about 1000 s within a $w = 100$ μm wide channel. It requires a 10 cm long downstream distance to completely mix even if the flow velocity is only 100 μm/s. The dimensionless Péclet number, $Pe = Uw/D$, provides an indication of the relative importance of diffusion and convection. Many designs have been exploited to enhance mixing in the microfluidic devices, in terms of passive and active modes (Nguyen and Wu, 2005). Passive mixing is realized by transverse flows induced by special geometries embedded in microchannels like grooves, rivets, or posts, or local circulations induced by heterogeneous surface pattern in electrokinetic flows, which requires no external forces. On the other hand, active mixing uses the flow disturbance generated by external fields such as acoustics, pressure, temperature, or electrohydrodynamics.

It is well known that the continuum theory in the Navier–Stokes equations only validates when the mean free path of the molecules is smaller than the characteristic length scale of the flow field. Otherwise, the fluid will no longer be in thermodynamic equilibrium and the linear relationship between the shear stress and rate of shear strain cannot be applied. The commonly used no-slip boundary condition at the fluid–solid interface is not fully valid, and a slip length has to

be introduced,

$$\Delta u|_w = u_{\text{fluid}} - u_{\text{wall}} = L_s \left.\frac{\partial u}{\partial y}\right|_w, \tag{9}$$

where $\Delta u|_w$ is the tangential velocity at the solid wall, L_s is the constant slip length determining the degree of slip, and $\partial u/\partial y|_w$ is the strain rate computed at the wall. It should be noted that so far there is no well-established theory for treating slip boundary at liquid–solid interface in small scales.

Fortunately, for normal liquid flows with the characteristic scale above 10 nm, the continuum assumption still holds practically. For example, modeling and simulation of electrokinetic flow, based on the classical Poisson–Boltzmann equations and the continuum Navier–Stokes equations, have explained many experimental results and guided the design of lab-on-a-chip systems. However, as the device scale shrinks further to several nanometers, or if the local effects such as surface roughness of molecular size and ion-surface interaction must be considered, one needs to resolve the atomistic details of the flow because these effects are neglected in the classical continuum theory. One example is the fluid density. Continuum theory assumes that the density does not vary significantly over intermolecular distance, but fluctuations of density in the vicinity of the solid surface have been confirmed by molecular dynamics simulation (Travis and Gubbins, 2000) and experiment (Cheng et al., 2001). Therefore, molecular-based computer simulations, mainly molecular dynamics (MD) method and direct simulation Monte Carlo (DSMC) method, are necessary for improving our understanding of the flows at these scales.

3. Simulation models

There are two basic models of simulating a flow field: the continuum model and the molecular model, as classified in Fig. 1 (Gad-el-Hak, 1999). The continuum model, in form of the Navier–Stokes equations, is able to describe the microfluidic phenomena where the channel sizes are in the micrometer range. As the length scale decreases further to naonometer range, the continuum assumption begins to break down and molecular models are needed to address the effects of the discrete particles: molecules, atoms, ions, and electrons.

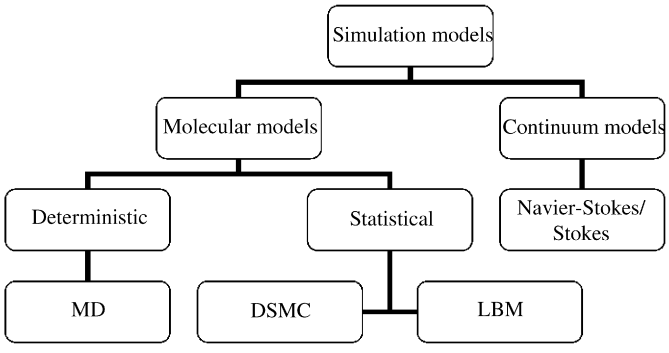

Fig. 1. Classification of the simulation models (adapted from Gad-el-Hak, 1999).

3.1. Navier–Stokes/Stokes simulation

Computational fluid dynamics (CFD) based on the continuum Navier–Stokes equations (Eq. (1)) has long been successfully used in fundamental research and engineering design in different fluid related areas. Naturally, it becomes the first choice for the simulation of microfluidic phenomena in lab-on-a-chip devices and is still the most popular simulation model to date. Due to the non-linearity arising from the convention term, Eq. (1) must be solved numerically by different discretization schemes, such as finite element method, finite difference method, finite volume method, or boundary element method. Besides, there are a variety of commercially available CFD packages that can be less or more adapted to model microfluidic processes (e.g., COMSOL (http://www.femlab.com), CFD-ACE+ (http://www.cfdrc.com), Coventor (http://www.coventor.com), Fluent (http://www.fluent.com), and Ansys CFX(http://www.ansys.com)). For majority of the microfluidic flows, *Re* number is always very small and thus the flows are Stokes type. The full Navier–Stokes equations thus can be linearized as Stokes equations, which greatly reduces the computational cost. The Navier–Stokes/Stokes equations, coupled with other equations, have been applied in study of many kinds of phenomena in the microfluidic systems: electrokinetic flow with Poisson–Boltzmann equation, species transportation with species transport equation, chemical reaction with reaction equation, and thermal analysis with heat transfer equation.

3.2. Molecular dynamics simulation

Molecular dynamics (MD) method was first used in thermodynamics, physical chemistry, and average thermochemical properties of gases, liquids, and solid (Alder and Wainwright, 1959; Allen and Tildesley, 1987; Koplik and Banavar, 1995). It has been recently applied to simulate the fluid and solid behavior in nanoscale (Xu et al., 1999; Crozier et al., 2001; Werder et al., 2001; Liu et al., 2004; Ho et al., 2006).

The basic idea of the MD method is straightforward: atoms or molecules are described as a system of interacting material points, whose motion is determined dynamically by a vector of instantaneous positions and velocities. The velocities $\mathbf{v}_i = (v_{x,i}, v_{y,i}, v_{z,i})$ and positions $\mathbf{r_i} = (x_i, y_i, z_i)$of the single atoms evolve according to Newton's law of motion,

$$m_i \frac{\partial \mathbf{v}_i}{\partial t} = \sum_{j \neq i} \nabla V(r_{ij}),$$
$$\frac{\partial \mathbf{r}_i}{\partial t} = \mathbf{v}_i(t), \tag{10}$$

where m_i is the mass and $V(r_{ij})$ is the interaction potential that models the physics of the system under consideration. Among a wide range of potentials employed in MD simulations, the Lennard–Jones 12-6 potential is typically used to represent

inter-atomic interactions,

$$V(r_{ij}) = 4\varepsilon\left[\left(\frac{\sigma}{r_{ij}}\right)^{12} - \left(\frac{\sigma}{r_{ij}}\right)^{6}\right], \tag{11}$$

where r_{ij} is the distance between atoms i and j, ε is the energy scale, and σ is the Lennard–Jones diameter. The set of Eq. (10) can be integrated in time, with initial conditions and specified boundary conditions. MD simulations are usually employed for homogeneous system where periodic boundary conditions are used. However, sometimes it is also necessary to impose arbitrary non-periodic boundary conditions. For example, interactions between the liquid and solid walls can be taken into account by adding different wall atoms, either fixed on a lattice or coupled to a lattice with large spring constant. Moreover, while the systems are conventionally treated as equilibrium systems, many phenomena are inherently non-equilibrium in nature and evolve with time, which requires non-equilibrium molecular dynamics (NEMD) methods.

Werder et al. (2001) conducted parallel MD simulations to investigate the wetting behavior of water droplets confined in carbon nanotubes and found that pure water showed a non-wetting behavior in nanotubes. Kalra et al. (2003) used MD to study osmotically driven transport of water molecules through hexagonally packed carbon nanotube membranes and revealed several distinct features of the nanoflows. The thermal fluctuations become significant at the nanoscale and the flow is stochastic in nature. The flow also appears frictionless and is limited mainly by the barrier at the inlet and outlet of the nanotube. Yeh and Hummer (2004) studied the electrophoresis of single-stranded RNA molecule through 1.5 nm wide pore of carbon nanotube membranes using MD simulations. They found that translocation kinetics of RNA through nanotube membranes is sequence-dependent, which suggests the possibility of extracting sequence information from synthetic-pore translocation data. MD simulations have been also applied in the study of ion (Joseph et al., 2003) and polymer (Wei and Srivastava, 2003) transport in nanotubes. Barrat and Bocquet (1999) applied NEMD to simulate Couette flow and Poiseuille flow on surfaces with contact angle reaching 140° and found a slip length of 30 molecular diameters (about 10 nm).

3.3. Direct simulation Monte Carlo (DSMC) method and lattice-Boltzmann method (LBM)

MD simulations are highly inefficient for dilute fluid where the molecular interactions are infrequent. Alternative statistical approaches, such as DSMC or LBM, are more suitable for dealing with such a situation. DSMC is a direct particle simulation method based on kinetic theory and its basic idea is to track a large number of statistically representative particles (Bird, 1978, 1994). Unlike exactly calculating collisions in MD simulations, DSMC models collisions stochastically using scattering rates and postcollision velocity distributions based on kinetic theory. DSMC simulations are not correct at atomic scale, but they are accurate at scales smaller than mean free path. Most of DSMC methods are based on the following Boltzmann equation (Oran et al., 1998):

$$\frac{\partial nf}{\partial t} + \mathbf{c}\cdot\frac{\partial nf}{\partial \mathbf{r}} + \mathbf{F}\cdot\frac{\partial nf}{\partial \mathbf{c}} = \int_{-\infty}^{\infty}\int_{0}^{4\pi} n^2(f^* f_1^* - f f_1) \times c_r \sigma \,\mathrm{d}\Omega\,\mathrm{d}\mathbf{c}_1, \tag{12}$$

where nf is the product of the number density n and the velocity distribution function f, $\mathbf{c}$ is the molecular velocity vector, c_r is the relative molecular speed, $\mathbf{F}$ is an external force, the superscript * denotes postcollision values, f and f_1 represent two different kinds of molecules, σ is the collision cross section, and Ω is the solid angle. The right-hand side term of Eq. (12) represents the collision of molecules. In the DSMC simulations, the physical flow domain is discretized into a grid of cells, structured or unstructured. The size of the cells should be sufficiently fine so that the change of flow properties across the cell is small. The time step is chosen so that the molecules do not move across more than one cell during a time step. With initial conditions and imposed boundary conditions, Eq. (12) can be numerically solved. The macroscopic flow parameters, such as density, velocity, and temperature, are obtained by averaging the corresponding velocity functions over all particles in a single cell. The DSMC method has been used successfully in the rarefied gas flows for several decades, and recently has been used to study microflow (mainly gas) in MEMS devices (Oh et al., 1997; Cai et al., 2000; Wang and Li, 2003). The DSMC method is designed based on the interaction features of gaseous molecules, i.e., the mean free path is much larger than the molecular size itself. Therefore, the application of the DSMC in liquid micro/nanofluidics is not popular since the liquid molecules, unlike the gaseous molecules, are close to each other.

Recently, a Lattice-Boltzmann method (LBM) has been developed to simulate flows in microchannels based on kinetic equations and statistical physics. In LBM, the motion of the fluid is modeled by a lattice Boltzmann equation for the distribution function of the fluid molecules. The discrete velocity Boltzmann equation corresponding to the Navier–Stokes equations can be written as

$$\frac{\partial f}{\partial t} + \mathbf{c}\cdot\nabla f = \Omega + F, \tag{13}$$

where f is the single-particle distribution function for particles moving at velocity $\mathbf{c}$, F is the external force term, and Ω is collision operator representing the change rate resulting from collisions in f. The most commonly used collision operator is the BGK (Bhatnagar–Gross–Krook) model which uses a single relaxation time approximation,

$$\Omega(f(\mathbf{x},t)) = -\frac{f(\mathbf{x},t) - f^{\mathrm{eq}}(\mathbf{x},t)}{\tau}. \tag{14}$$

The appropriately chosen equilibrium distribution, denoted by f^{eq}, depends on the local fluid variables, and $1/\tau$ is the rate of approach to this equilibrium.

The intrinsic kinetic nature of the LBM makes it an ideal choice for microfluidics where both macroscopic and microscopic effects are important. The LBM has comparable

computing efficiency to a Navier–Stokes solver yet has the potential of providing accurate results beyond the slip-flow regime. Moreover, external force field (e.g., applied electric field) can be more easily added to the lattice Boltzmann equation than to the Navier–Stokes equations and therefore several groups have applied the LBM to study electrokinetic flows in microfluidic devices (Horbach and Frenkel, 2001; Guo et al., 2005; Wang et al., 2006) and even in nanochannels (Melchionna and Succi, 2003).

3.4. Multiscale simulation

MD simulations have already become a powerful tool for studying nanoscale physical phenomena. However, the length and time scales that MD can probe are still very limited (tens of nanosecond and a few nanometers). For example, nanoscale flows are often a part of larger scale devices that could contain both nanochannels and microfluidic domains. The dynamics of these systems depends on the intimate connection of different scales from nanoscale to microscale and beyond. MD simulation cannot simulate the whole systems due to its prohibitive computational cost, whereas continuum Navier–Stokes simulation cannot elucidate the details in the small scales. These limitations and the practical needs arising from the study of multiscale problems have motivated research on multiscale simulation techniques that bridge a wider range of time and length scales with the minimum loss of information (Liu et al., 2004; Delgado-Buscalioni and Coveney, 2004). A hybrid molecular-continuum can make such multiscale computation feasible. A molecular-based method, such as MD for liquid or DSMC for gas, is used to describe the molecular details within the desired, localized subdomain of the large system; a continuum method, such as finite element or finite volume based Navier–Stokes/Stokes simulation, is used to describe the continuum flow in the remainder of the system. Such hybrid method can be applied to solve the multiscale phenomena in gas, liquid, or solid.

The key issue of the multiscale simulations is the coupling (exchanging information) between the molecular scale and the continuum scale. There are two classes of coupling scheme for liquids: direct flux exchange (O'Connell and Thompson, 1995; Delgado-Buscalioni and Coveney, 2003) and the domain decomposition method (Schwartz alternating method) (Hadjiconstantinou, 1999). O'Connell and Thompson's scheme implemented a finite overlap region between the molecular domain and continuum domain to avoid sharp density oscillation and therefore allow two solutions to relax before coupled together. Several extensions of the model have been made but without much improvements on outputs (Nie et al., 2004; Cui et al., 2006). The most critical problem with the model is how to determine the empirically coupling parameter. Recently, a dynamic coupling model was proposed to simultaneously calculate the free parameter without any a priori input in computation, which yielded satisfactory results for the Couette flow and the Stokes flow (Wang and He, 2007).

Various multiscale simulations have been used in studying the fluid flow with localized molecular characteristics. Aktas and Aluru (2002) applied a combined continuum/DSMC technique for multiscale analysis of microfluidic filters for particle trapping and sorting. Qiao and Aluru (2004) presented embedding multiscale simulation techniques for analysis of electroosmotic flow in nanochannels. The multiscale results were compared to direct MD simulations and found good agreement in ion distribution and velocity profile. Their simulations also indicated that the classical continuum theory significantly overestimates the average velocity at a high-bulk concentration. Werder et al. (2005) developed an MD simulation coupled to a continuum Navier–Stokes solver based on finite volume discretization. The two regions were combined through Schwarz alternating method to exchange information. They used this hybrid method to study the flow of liquid argon past a carbon nanotube, and found that the resulting flow field agreed with a fully molecular reference solution.

4. Examples of microfluidic and nanofluidic applications

In the above, we have reviewed some key electrokinetic microfluidic phenomena and the computational methods used to study these phenomena over different length scales. The following are several examples of applications of electrokinetically controlled micro/nanofluidic devices that take advantages of these phenomena at different scales.

4.1. Enhanced micromixing using heterogeneous surface

The electrokinetically driven flows have expanded the potential of surface chemistry as a means of mixing enhancement. The microscale flow transport strongly depends on both the local and global surface properties. Electroosmotic flow tends to be exceptionally sensitive to the heterogeneities in the surface charge that affect the local electrokinetic body force and lead to induced pressure forces or localized flow circulation. Ajdari conducted a series of analytical studies examining these effects on electroosmotic flows over non-uniform surfaces (Ajdari, 1995) and transverse effects using channel shape and charge-density modulations (Ajdari, 1996, 2002). Erickson and Li (2003) conducted 3D numerical simulations based on a coupled solution to the Nernst–Planck, Poisson and Navier–Stokes equations for electroosmotic flow over periodically repeating non-uniform surface ζ potential pattern. The simulations revealed a distinct 3D flow structure that, depending on the degree of heterogeneity, varies from a weak circulation perpendicular to the electric field to a fully circulatory flow pattern. Therefore, it is natural to consider using such effects from heterogeneous surface to enhance mixing in the microfluidic systems.

Biddiss et al. (2004) experimentally visualized the effects of surface charge patterning and developed an optimized electrokinetic micromixer applicable to the low *Re* number flows. The surface charge patterning in a PDMS microchip was realized by polyelectrolyte coating. To facilitate optimization of surface charge patterning, a finite element code was adapted to simulate the experimental conditions and surface charge heterogeneities.

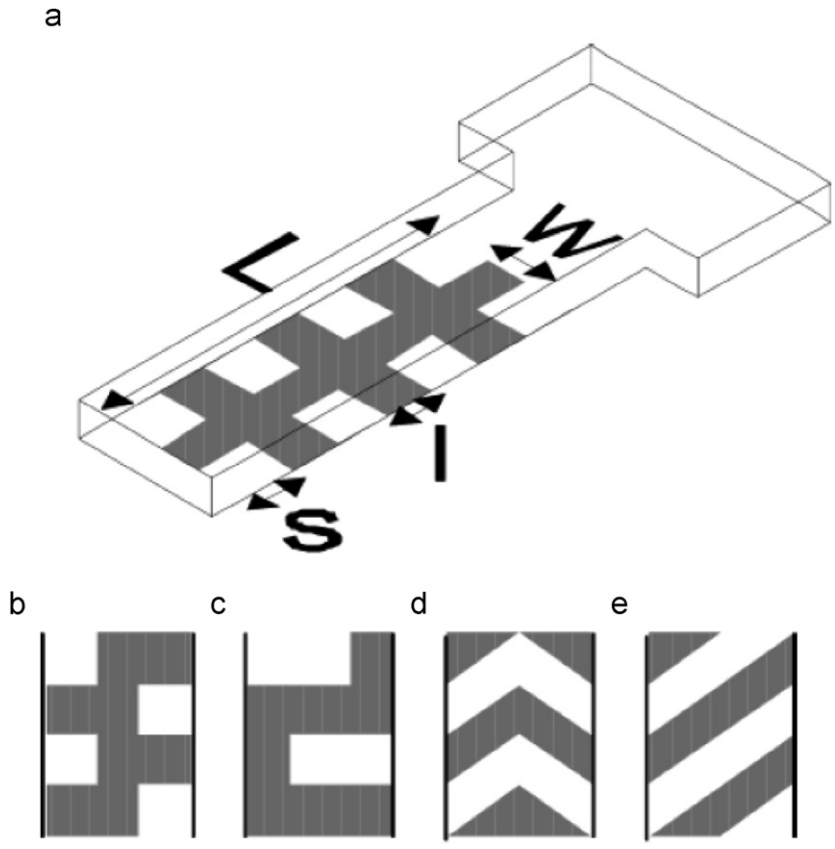

Fig. 2. Different surface charge patterning configuration (Biddiss et al., 2004).

Fig. 2 shows the different surface patterning configurations. The flow field was then visualized by adding fluorescence dye. Fig. 3 shows the flow fields obtained experimentally and numerically for the homogeneous and heterogeneous surface. It was found that using the optimized micromixer, mixing efficiencies were improved between 22% and 68% for electric fields ranging from 70 to 555 V/cm. For producing a 95% mixture, such improvement equals to a possible decrease in the mixing channel length of up to 88% for Péclet numbers between 190 and 1500.

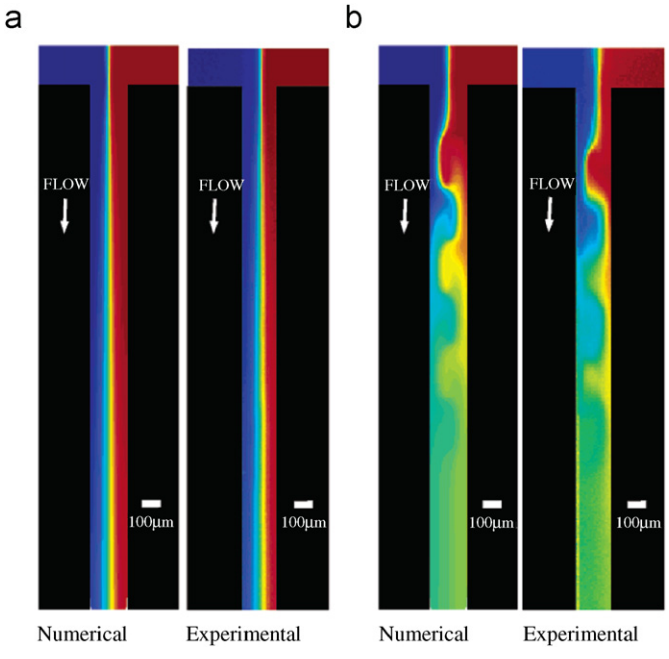

Fig. 3. Images of steady-state species transport under an electric field of 280 V/cm for (a) the homogeneous microchannel and (b) the heterogeneous microchannel with six offset staggered patches (Biddiss et al., 2004).

4.2. Particle/cell separation using DC-DEP

DEP has been widely used in on-chip particle or cell separation (Gascoyne and Vykoukal, 2002; Hughes, 2002,). Highly non-uniform electric field at length scale comparable to particle/cell size is needed to be generated. In the AC-DEP application, an array of metal electrodes is usually embedded inside a microchannel network to generate such non-uniform electric field, which requires relatively complex microfabrication procedure. On the other hand, the same effect can be achieved by a DC electric field by specially designed structures, such as obstructions or hurdles using electrically insulating materials. Cummings and Singh (2003) developed an insulator-based DEP device consisting of an array of insulating rods in a microchannel by which DEP trapping of 200 nm polystyrene particles was realized. Lapizco-Encinas et al. (2004) demonstrated selective trapping of polystyrene particles, live *E. coli*, and dead *E. coli*

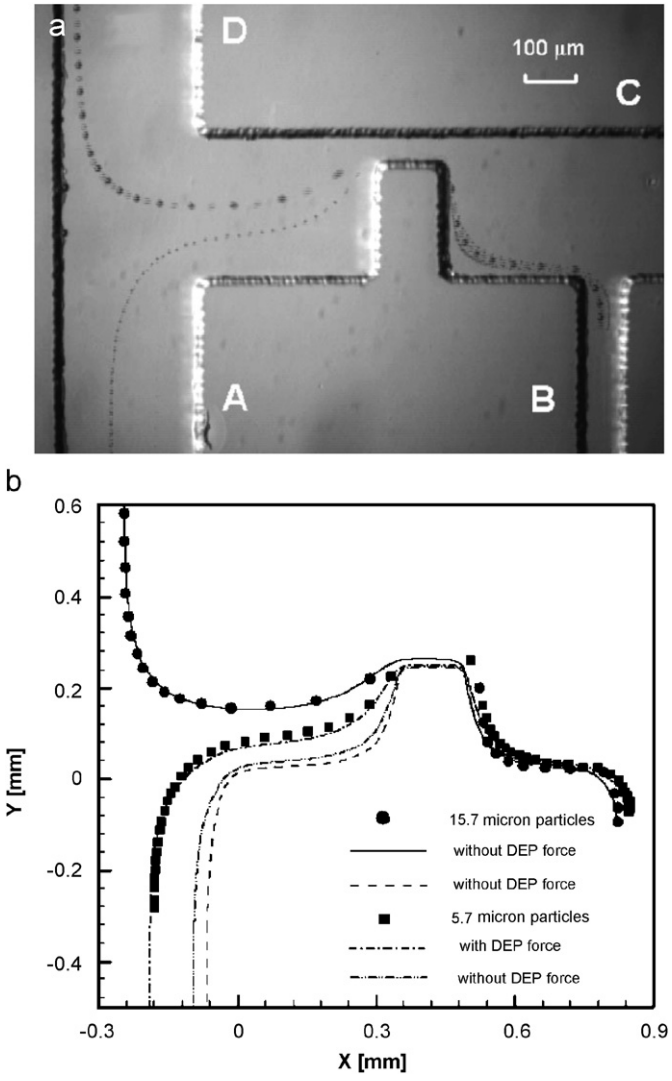

Fig. 4. Separation of 5.7 and 15.7 μm particles at 500 V voltage level. Applied voltages at different electrodes: $V_A=54$ V, $V_B=244$ V, $V_C=502$ V, $V_D=0$ V; (a) superposed particle trajectories; (b) comparison of the simulation results and the experimental data (Kang et al., 2006).

in arrays of insulating posts using DC electric fields. However, no one has shown the separation of particles or cells by size in DC electrokinetic flow by DC-DEP.

Kang et al. (2006) designed a novel technique using DC-DEP to separate polystyrene microparticles by their sizes. The key structure of this design is an insulating block between the input and separation branches to form a gap with comparable size to cell diameter, which can generate a local non-uniform electric field. The particle trajectories are deflected by the DEP force around the block; large and small particles are diverted into different streams and thus separated, as shown in Fig. 4. A noticeable advantage of this device is that the different size particles can be separated and electrokinetically transported simultaneously by the same DC electric field, which greatly simplified the peripheral equipment for flow control. Moreover, by adjusting the applied voltage at the ends of different branches, a mixture of microparticles of two different sizes can be continuously separated, without a redesign of the microchannel configurations.

4.3. Novel separation techniques for DNA

DNA separation is essential for the DNA fingerprinting, genome sequencing, and other numerous genetic assays. Efforts to realize DNA separation in micro-devices have led to advances in microcapillary electrophoresis and the development of novel separation strategies. DNA fragments of different sizes may have similar electrophoretic mobilities. Gel electrophoresis is the standard method for separation of DNA by length. However, it can only separate efficiently DNA molecules up to around 40 kbp, above which the mobility becomes independent of the size due to DNA stretching. Slab gel pulsed-field gel electrophoresis (PFGE) can be used to separate longer double-stranded DNA (dsDNA) using time-varying electric voltages, but the process usually takes several days and weeks (Cox et al., 1990; Han and Craighead, 2000). Moreover, it could be difficult to introduce and integrate gel matrix into the microfabricated devices. Many researchers have proposed novel separation schemes that utilize directly the hierarchical structures in micro/nanofluidic platforms. Han and Craighead (2000) developed a rectangle nanofluidic channel, consisting of alternating narrow and wider regions, to separate long DNA molecules. Such a configuration causes size-dependent trapping of DNA at the onset of a constriction and creates electrophoretic mobility differences, thus enabling efficient separation without the use of a gel matrix or pulsed electric fields. It is normally difficult to introduce long DNA molecules into nanofluidic channels directly from macroscale due to steep entropic barrier from stretching of DNA molecules. Cao et al. (2002) used optical lithography to fabricate continuous spatial gradient structures that can smoothly narrow the cross section of a volume from the micron to the nanometer scale, significantly alleviating the effects of entropic barrier at the nanochannel inlet. Internal conformational entropy is one of the dominant properties of DNA molecules. If a DNA molecule undergoes a constriction much less than its radius of gyration, it has to be deformed from its equilibrium shape to fit into the constriction. Since the deformation is entropically unfavorable, it tends to return back to its original shape once the external driving force disappears. This effect is called entropic trapping. Turner et al. (2002) described a separation strategy based on the principle of entropic trapping. Their quasi-2D chip consists of two different regions: a plane region and region containing a dense array of nanopillars each with a diameter of 35 nm and a height of 60 nm. Under the influence of an applied electric field, the DNA molecules begin to migrate towards the pillared regions from the original plane region, as shown in Fig. 5. After certain time, smaller DNA molecules will enter the pillared region entirely, whereas larger DNA molecules will enter partially. When the electric field is turned off, the partially entered longer DNA molecules quickly recoil in the plane region in order to maximize their conformational entropy. Molecules that are completely present in either of the two regions do not experience any force since

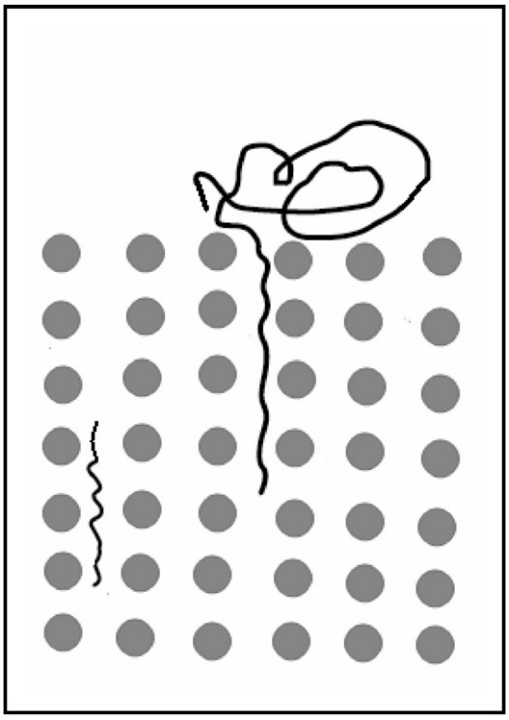

Fig. 5. A schematic top view of the device from Turner et al. (2002). The gray circles represents nanopillars with a diameter of 35 nm. DNA molecules enter the dense pillar region under an applied electric field (adapted from Turner et al., 2002).

their entropies are uniform. Therefore, DNA molecules with different sizes can be effectively separated.

5. Conclusions

We have reviewed the multiscale phenomena in microfluidic and nanofluidic devices, with focus on electrokinetics. We have compared different numerical models used in computational microfluidics and nanofluidics, including the relevant underlying concepts and principles. Several application examples have been shown to illustrate how to use the size effects in the small devices.

As advancements in microfabrication techniques allow for further shrinking lab-on-a-chip devices from the micron regime to the nanometer regime, much of the non-traditional physics is still to be discovered and many exciting applications of lab-on-a-chip devices are yet to be exploited. For example, fast sequencing of DNA strands with a nanopore device needs the knowledge of the conformations of DNA inside the pore in atomic detail. Due to difficulties associated with the nanoscale experiments, molecular-based modeling and simulations will play a more and more important role in the development and optimization of such devices. The computer models must be able to cover length scale from nanometer to micrometer, and time scale from femtosecond to microsecond. Therefore, considerable research effort should be put to construct the foundations for the multiscale methodology and to develop computational capability to realize such multiscale simulations. Meanwhile, it is also essential to develop novel experimental techniques for direct measurement and visualization of flow fields and molecular transport in the nanoscale. Such techniques will not only generate first-hand observation in nanometer regime, but also provide validation and improvement for the molecular-based models.

Acknowledgments

The authors are indebted to the support from a start-up grant from the School of Engineering, Vanderbilt University.

References

Ajdari, A., 1995. Electro-osmosis on inhomogeneously charged surfaces. Physical Review Letters 75, 755–758.

Ajdari, A., 1996. Generation of transverse fluid current and forces by an electric field: electro-osmosis on charge-modulated and undulated surfaces. Physical Review E 53, 4996–5005.

Ajdari, A., 2001. Pumping liquids using asymmetric electrode arrays. Physical Review E 61, R45.

Ajdari, A., 2002. Transverse electrokinetic and microfluidic effects in micropatterned channels: lubrication analysis for slab geometries. Physical Review E 65, 016301.

Alder, B.J., Wainwright, T.E., 1959. Studies in molecular dynamics. I. General method. Journal of Chemical Physics 31, 459–466.

Allen, M.P., Tildesley, D.J., 1987. Computer Simulation of Liquids. Clarendon Press, Oxford, UK.

Anderson, J.L., 1989. Colloid transport by interfacial forces. Annual Review of Fluid Mechanics 21, 61–99.

Aktas, O., Aluru, N.R., 2002. A combined continuum/DSMC technique for multiscale analysis of microfluidic filters. Journal of Computational Physics 178, 342–372.

Auroux, P.-A., Iossifidis, D., Reyes, D.R., Manz, A., 2002. Micro total analysis systems. 2. Analytical Standard Operations and Applications 74, 2637–2652.

Barany, S., Mishchuk, N.A., Prieve, D.C., 1998. Superfast electrophoresis of conducting dispersed particles. Journal of Colloid and Interface Science 207, 240–250.

Barrat, J.L., Bocquet, L., 1999. Large slip effect at a nonwetting fluid–solid interface. Physical Review Letters, 4671–4674.

Bazant, M.Z., Squires, T.M., 2004. Induced-charge electrokinetic phenomena: theory and microfluidic applications. Physical Review Letters 92, 066101.

Ben, Y., Chang, H.-C., 2002. Nonlinear Smoluchowski slip velocity and micro-vortex generation. Journal of Fluid Mechanics 461, 229–238.

Ben, Y., Demekhin, E.A., Chang, H.-C., 2004. Nonlinear electrokinetics and "superfast" electrophoresis. Journal of Colloid and Interface Science 276, 483–497.

Biddiss, E., Erickson, D., Li, D., 2004. Surface charge enhanced micro-mixing for electrokinetic flows. Analytical Chemistry 76, 3208–3213.

Bird, G.A., 1978. Monte Carlo simulation of gas flows. Annual Review of Fluid Mechanics 10, 11–31.

Bird, G.A., 1994. Molecular Gas Dynamics and the Direct Simulation of Gas Flows. Clarendon Press, Oxford, UK.

Burgreen, D., Nakache, F.R., 1964. Electrokinetic flow in ultrafine capillary silts. Journal of Physical Chemistry 68, 1084–1091.

Cai, C., Boyd, I.D., Fan, J., Candler, G.V., 2000. Direct simulation methods for low-speed microchannel flows. Journal of Thermophysics and Heat Transfer 14, 368–378.

Cao, H., Tegenfeldt, J.O., Austin, R.H., Chou, S.Y., 2002. Gradient nanostructures for interfacing microfluidics and nanofluidics. Applied Physics Letters 81, 3058–3060.

Cheng, L., Fenter, P., Nagy, K.L., Schlegel, M.L., Sturchio, N.C., 2001. Molecular-scale density oscillations in water adjacent to a mica surface. Physical Review Letters 87, 156103.

Cox, E.C., Vocke, C.D., Walter, S., et al., 1990. Electrophoretic karyotype for Dictyostelium discoideum. Proceedings of the National Academy of Science USA 87, 8247–8251.

Crozier, P.S., Henderson, D., Rowley, R.L., Busath, D.D., 2001. Model channel ion currents in NaCl-extended simple point charge water solution with applied-field moleculary dynamics. Biophysical Journal 81, 3077–3089.

Cui, J., He, G.W., Qi, D.W., 2006. A constrained particle dynamics for continuum-particle hybrid method in micro- and nano-fluidics. Acta Mechanica Sinica 22, 6.

Cummings, E.B., Singh, A.K., 2003. Dielectrophoresis in microchips containing arrays of insulating posts: theoretical and experimental results. Analytical Chemistry 75, 4724–4731.

Cummings, E.B., Griffiths, S.K., Nilson, R.H., Paul, P.H., 2000. Conditions for similitude between the fluid velocity and electric field in electroosmotic flow. Analytical Chemsitry 72, 2526–2532.

Delgado-Buscalioni, R., Coveney, P.V., 2003. Continuum-particle hybrid coupling for mass, momentum, and energy transfers in unsteady flow. Physical Review E 67, 046704.

Delgado-Buscalioni, R., Coveney, P.V., 2004. Hybrid molecular-continuum fluid dynamics. Philosophical Transactions of the Royal Society A 362, 1639–1654.

Erickson, D., Li, D., 2003. Three-dimensional structure of electroosmotic flows over heterogeneous surfaces. Journal of Physical Chemistry B 107, 12212–12220.

Dukhin, S.S., 1991. Electrokinetic phenomena of the second kind and their applications. Advances in Colloid and Interface Science 35, 173–196.

Erickson, D., 2005. Towards numerical prototyping of labs-on-chip: modeling for integrated microfluidic devices. Microfluidics and Nanofluidics 1, 301–318.

Erickson, D., Li, D., 2003. Three dimensional structure of electroosmotic flow over periodically heterogeneous surface patterns. Journal of Physical Chemistry B 107, 12212–12220.

Erickson, D., Li, D., 2004. Integrated microfluidic devices. Analytica Chimica Acta 507, 11–26.

Gad-el-Hak, M., 1999. The fluid mechanics of microdevices-the Freeman scholar lecture. Journal of Fluids Engineering 121, 5–33.

Gascoyne, P.R.C., Vykoukal, J., 2002. Particle separation by dielectrophoresis. Electrophoresis 23, 1973–1983.

Ghosal, S., 2004. Fluid mechanics of electroosmotic flow and its effect on band broadening in capillary electrophoresis. Electrophoresis 25, 214–228.

Guo, Z., Zhao, T.S., Shi, Y., 2005. A lattice Boltzmann algorithm for electro-osmotic flows in microfluidic devices. Journal of Chemical Physics 122, 144907.

Hadjiconstantinou, N.G., 1999. Hybrid atomistic-continuum formulations and the moving contact-line problem. Journal of Computational Physics 154, 245–265.

Han, J., Craighead, H.G., 2000. Separation of long DNA molecules in a microfabricated entropic trap array. Science 288, 1026–1029.

Herr, A.E., Molho, J.I., Santiago, J.G., Mungal, M.G., Kenny, T.W., 2000. Electroosmotic capillary flow with nonuniform zeta potential. Analytical Chemistry 72, 1053–1057.

Ho, C., Qiao, R., Heng, J.B., Chatterjee, A., Timp, R.J., Aluru, N.R., Timp, G., 2006. Electrolytic transport through a synthetic nanometer-diameter pore. Proceedings of the National Academy of Science USA 102, 10445–10450.

Horbach, J., Frenkel, D., 2001. Lattice-Boltzmann method for the simulation of transport phenomena in charged colloids. Physical Review E 64, 061507.

Hu, G., Gao, Y., Sherman, P.M., Li, D., 2005. A microfluidic chip for heterogeneous immunoassay using electrokinetical control. Microfluidics and Nanofluidics 1, 346–355.

Hughes, M.P., 2002. Strategies for dielectrophoretic separation in laboratory-on-a-chip systems. Electrophoresis 23, 2569–2582.

Hunter, R.J., 1981. Zeta Potential in Colloid Science, Principals and Applications. Academic Press, New York, USA.

Johns, T.B., Washizu, M., 1996. Multipolar dielectrophoretic and electrorotation theory. Journal of Electrostatics 37, 121–134.

Joseph, S., Mashl, R.J., Jakobsson, E., Aluru, N.R., 2003. Electrolytic transport in modified carbon nanotubes. Nano Letters 3, 1399–1403.

Kalra, A., Garde, S., Hummer, G., 2003. Osmotic water transport through carbon nanotube membranes. Proceedings of the National Academy of Science, USA 100, 10175–10180.

Kang, K.H., Kang, Y., Xuan, C., Li, D., 2006. Continuous separation of microparticles by size with direct current-dielectrophoresis. Electrophoresis 27, 694–702.

Kock, M., Evans, A., Brunnschweiler, A., 2000. Microfluidic Technology and Applications. Research Studies Press, Hertfordshire, UK.

Koplik, J., Banavar, J.R., 1995. Continuum deductions from molecular hydrodynamics. Annual Review of Fluid Mechanics 27, 257–292.

Lapizco-Encinas, B.H., Simmons, B.A., Cummings, E.B., Fintschenko, Y., 2004. Dielectrophoretic concentration and separation of live and dead bacteria in an array of insulators. Analytical Chemistry 76, 1571–1579.

Lee, J.S.H., Hu, Y., Li, D., 2005. Electrokinetic concentration gradient generation using a converging–diverging microchannel. Analytica Chimica Acta 543, 99–108.

Li, D., 2004. Electrokinetics in Microfluidics. Academic Press, New York, USA.

Liu, W.K., Karpov, E.G., Zhang, S., Park, H.S., 2004. An introduction to computational nanomechanics and materials. Computer Methods in Applied Mechanics and Engineering 193, 1529–1578.

Manz, A., Graber, N., Widmer, H.M., 1990. Miniaturised total chemical analysis systems: a novel concept for chemical sensing. Sensors and Actuators B 1, 244–248.

Melchionna, S., Succi, S., 2003. Electrorheology in nanopores via lattice Boltzmann simulation. Journal of Chemical Physics 120, 4492–4497.

Morrison Jr., F.A., 1970. Electrophoresis of a particle of arbitrary shape. Journal of Colloid and Interface Science 34, 210–214.

Nguyen, N.-T., Wu, Z., 2005. Micromixers-a review. Journal of Micromechanics and Microengineering 15, R1–R6.

Nie, X.B., Chen, S.Y., E, W.N., Robbins, M.O., 2004. A continuum and molecular dynamics hybrid method for micro- and nano-fluid flow. Journal of Fluid Mechanics 500, 55–64.

O'Connell, S.T., Thompson, P.A., 1995. Molecular dynamics-continuum hybrid computations: a tool for studying complex fluid flow. Physical Review E 52, R5792–R5795.

Oh, C.K., Oran, E.S., Sinkovits, R.S., 1997. Computations of high-speed, high Knudsen number microchannel flows. Journal of Thermophysics and Heat Transfer 11, 497–505.

Oran, E.S., Oh, C.K., Cybyk, B.Z., 1998. Direct simulation Monte Carlo: recent advances and applications. Annual Review of Fluid Mechanics 30, 403–441.

Paegel, B.M., Emrich, C.A., Wedemayer, G.J., Scherer, J.R., Mathies, R.A., 2002. High throughput DNA sequencing with a microfabricated 96-lane capillary array electrophoresis bioprocessor. Proceedings of the National Academy of Science USA 99, 574–579.

Pohl, H.A., 1978. Dielectrophoresis. Cambridge University Press, New York, USA.

Probstein, R.F., 1994. Physicochemical Hydrodynamics. Willey, New York, USA.

Qiao, R., Aluru, N.R., 2002. Ion concentrations and velocity profiles in nanochannel electroosmotic flows. Journal of Chemical Physics 118, 4692–4701.

Qiao, R., Aluru, N.R., 2004. Multiscale simulation of electroosmotic transport using embedding techniques. International Journal of Multiscale Computational Engineering 2, 173–188.

Ren, C.L., Li, D., 2005. Improved understanding of the effect of electrical double layer on pressure-driven flow in microchannels. Analytica Chimica Acta 531, 15–23.

Ren, L., Sinton, D., Li, D., 2003. Numerical simulation of microfluidic injection processes in crossing microchannels. Journal of Micromechanics and Microengineering 13, 739–747.

Reyes, D.R., Iossifidis, D., Auroux, P.-A., Manz, A., 2002. Micro total analysis systems. 1. Introduction, theory, and technology. Analytical Chemistry 74, 2623–2636.

Ross, D., Gaitan, M., Locascio, L.E., 2001. Temperature measurement in microfluidic systems using a temperature-dependent fluorescent dye. Analytical Chemistry 73, 4117–4123.

Russel, W.B., Saville, D.A., Schowalter, W.R., 1989. Colloidal Dispersions. Cambridge University Press, Cambridge, UK.

Santiago, J.G., 2001. Electroosmotic flows in microchannels with finite inertial and pressure forces. Analytical Chemistry 73, 2353–2365.

Schmalzing, D., Belenky, A., Novotny, M.A., Koutny, L., Salas-Solano, O., EI-Difrawy, S., Adourian, A., Matsudaira, P., Ehrlich, D., 2000. Microchip electrophoresis: a method for high-speed SNP detection. Nucleic Acids Research 28, e43.

Squires, T.M., Quake, S.R., 2005. Microfluidics: fluid physics at the nanoliter scale. Reviews of Modern Physics 77, 977–1026.

Stone, H.A., Stroock, A.D., Ajdari, A., 2004. Engineering flows in small devices: microfluidics toward a lab-on-a-chip. Annual Review of Fluid Mechanics 36, 381–411.

Taylor, J., Ren, C.L., 2005. Application continuum mechanics to fluid flow in nanochannels. Microfluidics and Nanofluidics 1, 356–363.

Tegenfeldt, J.O., Prinz, C., Cao, H., Huang, R.L., Austin, R.H., Chou, S.Y., Cox, E.C., Sturm, J.C., 2004. Micro- and nanofluidics for DNA analysis. Analytical and Bioanalytical Chemistry 378, 1678–1692.

Tian, H., Brody, L.C., Fan, S., Huang, Z., Landers, J.P., 2001. Capillary and microchip electrophoresis for rapid detection of known mutations by combing allele-specific DNA amplification with heteroduplex analysis. Clinical Chemistry 47, 173–185.

Travis, K.P., Gubbins, K.E., 2000. Poiseuille flow of Lennard–Jones fluids in narrow slit pores. Journal of Chemical Physics 112, 1984–1994.

Turner, S.W.P., Cabodi, M., Craighead, H.G., 2002. Confinement-induced entropic recoil of single DNA molecules in a nanofluidic structure. Physical Review Letters 88, 128103.

Wang, Y.C., He, G.W., 2007. A dynamic coupling model for hybrid atomistic-continuum computations. Chemical Engineering Science, this issue, doi:10.1016/j.ces.2006.12.093.

Wang, M., Li, Z., 2003. Nonideal gas flow and heat transfer in micro- and nano-channels using the direct simulation Monte Carlo method. Physical Review E 68, 046704.

Wang, S.-C., Lai, Y.-W., Ben, Y., Chang, H.-C., 2004. Microfluidics mixing by dc and ac nonlinear electrokinetic vortex flows. Industrial and Engineering Chemistry Research 43, 2902–2911.

Wang, J., Wang, M., Li, Z., 2006. Lattice Poisson–Boltzmann simulations of electro-osmotic flows in microchannels. Journal of Colloid and Interface Science 296, 729–736.

Wei, C., Srivastava, D., 2003. Theory of transport of long polymer molecules through carbon nanotube channels. Physical Review Letters 91, 235901.

Werder, T., Walther, J.H., Jaffe, R.L., Halicioglu, T., Noca, F., Koumoutsakos, P., 2001. Molecular dynamics simulation of contact angles of water droplets in carbon nanotubes. Nano Letters 1, 697–702.

Werder, T., Walther, J.H., Koumoutsakos, P., 2005. Hybrid atomistic-continuum method for the simulation of dense fluid flows. Journal of Computational Physics 205, 373–390.

Xu, L., Tsotsis, T.T., Sahimi, M., 1999. Nonequilibrium molecular dynamics simulation of transport and separation of gases in carbon nanopores. I. Basic results. Journal of Chemical Physics 111, 3252–3264.

Xu, F., Jabasini, M., Baba, Y., 2002. DNA separation by microchip electrophoresis using low-viscosity hydroxypropylmethylcellulose-50 solutions enhanced by polyhydroxy compounds. Electrophoresis 23, 3608–3614.

Xuan, X.C., Li, D., 2005. Focused electrophoretic motion and selected electrokinetic dispensing of particles and cells in cross-microchannels. Electrophoresis 26, 3552–3560.

Xuan, X.C., Xu, B., Sinton, D., Li, D., 2004. Electroosmotic flow with Joule heating effects. Lab on a Chip 4, 230–236.

Yeh, I.-C., Hummer, G., 2004. Nucleic acid transport through carbon nanotube membranes. Proceedings of the National Academy of Science USA 101, 12177–12182.

Zhang, J., He, G., Liu, F., 2006. Electro-osmotic flow and mixing in heterogeneous microchannels. Physical Review E 73, 056305.